Fine Grain Spectrum Analysis of Pulsed Microwave Amplifiers*

ROLAND F. KOONTZ†, MEMBER, IRE

Summary—With the advent of microwave transmitter systems requiring high spectral purity, it has become important to control the interline noise and modulation products in the fine grain spectrum of CW or pulsed microwave amplifiers. Some of the causes of interline noise and modulation in high-power microwave amplifiers such as klystrons, TWT's and coaxial triodes are reviewed in this paper. A spectrum analyzer capable of resolving interline noise and modulation products in CW or pulsed microwave spectrums is described. This analyzer has a dynamic range of better than 50 db and a resolution of less than 2 cps. Some typical measurements made on transmitters operating in the UHF and L-band regions are presented.

I. General

In THE design, construction and evaluation of high-power microwave amplifiers and their associated transmitter systems, a high degree of emphasis is currently being placed on the development of microwave amplifier systems which can amplify complex microwave pulse spectra without introducing noise or spurious modulation into the spectrum. The frequency spectrum of a periodic pulsed microwave signal consists of discrete energy lines with a frequency spacing equal to the pulse repetition frequency. For a rectangular pulse modulated on a fixed frequency carrier, the envelope of these lines will be a $(\sin x)/x$ function.

In many new radar systems today it is necessary to keep the energy distribution of these lines confined to a narrow frequency space with the interline frequency regions kept free of all noise and spurious modulation. To meet these requirements equipment capable of measuring spectrum line widths and inspecting interline frequency regions is required. Commerical panoramic spectrum analyzers on the market today do not have narrow enough resolution to resolve the line structure of most microwave pulse spectrums. They are limited in their resolution by the frequency instability of their internal sweeping and transfer oscillators and by the Q of their filters.

If transfer oscillator instability can be separated from the microwave pulsed signal, the signal can be transferred to a low frequency where a filter and sweeping circuit of reasonable Q and stablility can provide the necessary resolution. Using a coherent conversion system transfer oscillator instabilities can be eliminated. A coherent converter translates a very stable low-frequency source up to microwave frequency in several conversions using separate transfer oscillators. This microwave signal is used as the input signal to the device under test. The output spectrum of the device under test is reconverted to the low frequency using the same transfer oscillators as for the up conversion. This operation cancels any transfer oscillator instability from the spectrum output at the low frequency. With the pulse spectrum now transferred to a low-frequency base, it is possible to build filters which will resolve the individual spectrum lines and the interline frequency spaces.

An analyzer embodying these principles was constructed and used to evaluate several microwave amplifiers and transmitter systems. The analyzer contained a filter having a 3-db bandwidth of 2 cps. The signal-frequency stability imparted by the coherent conversion process was well within this filter bandwidth. Of the several UHF and L-band amplifiers tested with the analyzer, the most prominent cause of interline modulation was ac modulation based on power-line frequency and harmonics thereof. Mechanical vibration of devices using cavity resonators also contributed to interline modulation levels. No significant widening of the f_0 spectral line over the 2-cps width of the filter was observed in any of the amplifiers tested. PRF spectral lines, however, being dependent on pulse-repetition frequency stability were found to jitter considerably for all but very stable PRF rates. In the course of development of two transmitter systems, the analyzer was found very useful in detecting, isolating and correcting modulation problems which might otherwise have gone undetected until the final radar system integration period.

II. Frequency Spectrum Analysis

The frequency spectrum of a microwave pulse train can be represented by the Fourier series

$$H(f) = AFt_0\left[\sum_{n=-\infty}^{n=\infty} \delta[(f - f_0) - nF]\right] \cdot \frac{\sin(\pi t_0(f - f_0))}{\pi t_0(f - f_0)} \quad (1)$$

where $H(f)$ is the voltage distribution of the pulse train, and

A = pulse amplitude
t_0 = pulse width
F = pulse-repetition frequency
f_0 = carrier frequency.

The spectrum energy is concentrated in discrete lines separated in frequency by an interval (F). These discrete lines have voltage levels proportional to a $(\sin x)/x$ function. (See Fig. 1.)

The frequency function $H(f)$ is what is presented to

* Received April 26, 1962; revised manuscript received July 10, 1962.
† Missile and Surface Radar Div., Defense Electronic Products, RCA, Moorestown, N. J.

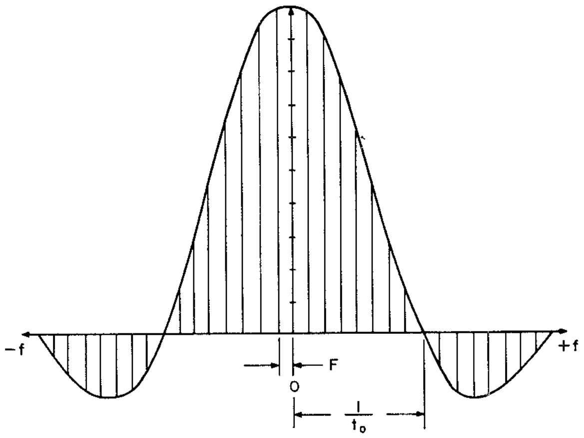

Fig. 1—Frequency spectrum of a rectangular pulse train.

the transmitter for amplification. To study the various modulation mechanisms within the transmitter which operate on this function, it will suffice to trace only one frequency line of the function $H(f)$ through the transmitter as all the lines will be modulated in a similar manner. Studying the modulation that occurs to this line will give a picture of the modulation occurring in the whole spectrum.

In (1) we choose the spectral line corresponding to $n=0$ as the line which will be traced through the amplifier chain.

$$H(f_0) = At_0F \qquad \text{for } n = 0. \tag{2}$$

This corresponds to the f_0 spectral line. All other spectral lines are smaller in magnitude than this line, hence the modulation occurring to this line will have larger absolute amplitude than modulation occurring to other lines. The time function corresponding to $H(f)$ is

$$f(t) = A_0' \operatorname{Cos}(2\pi f_0 t) \tag{3}$$

where

$$A_0' = At_0F. \tag{4}$$

Two forms of modulation are possible in the transmitter: amplitude modulation and angle modulation, the latter including phase modulation and frequency modulation.

A. Amplitude Modulation

The function (3) is amplified in the transmitter by an amplification factor K so that the output of the transmitter is

$$Kf(t) = KA_0' \operatorname{Cos}(2\pi f_0 t). \tag{5}$$

If for any reason K varies with time, amplitude modulation of $f(t)$ will occur.

$$K(t)f(t) = K(t)A_0' \operatorname{Cos}(2\pi f_0 t). \tag{6}$$

$K(t)$ may be divided into K_0, the fixed gain, and $k(t)$ the gain variation.

$$K(t) = K_0 + k(t). \tag{7}$$

$$K(t)f(t) = [K_0 + k(t)]A_0' \operatorname{Cos}(2\pi f_0 t). \tag{8}$$

$$K(t)f(t) = K_0A_0'\left[1 + \frac{k(t)}{K_0}\right] \operatorname{Cos} 2\pi f_0 t. \tag{9}$$

For a gain variation $k(t)$ represented by a sum of sinusoidal components

$$k(t) = \sum_{n=1}^{n=M} a_n \operatorname{Cos}(\rho_n t + \theta_n) \tag{10}$$

where ρ_n is the angular frequency of the nth component, and θ_n is the constant part of its phase.

$$K(t)f(t) = \underbrace{K_0A_0' \operatorname{Cos}(2\pi f_0 t)}_{f_0 \text{ line}} + \underbrace{A_0' \operatorname{Cos}(2\pi f_0 t)\left[\sum_{n=1}^{n=M} a_n \operatorname{Cos}(\rho_n t + \theta_n)\right]}_{\text{modulation lines}}. \tag{11}$$

Expanding the modulation line portion of the above expression

$$\begin{aligned} A_0'(\operatorname{Cos}(2\pi f_0 t))&\left[\sum_{n=1}^{n=M} a_n \operatorname{Cos}(\rho_n t + \theta_n)\right] \\ &= \frac{A_0'a_1}{2} \operatorname{Cos}[(2\pi f_0 + \rho_1)t + \theta_1] + \frac{A_0'a_1}{2} \operatorname{Cos}[(2\pi f_0 - \rho_1)t + \theta_1] + \cdots \\ &+ \underbrace{\frac{A_0'a_n}{2} \operatorname{Cos}[(2\pi f_0 + \rho_n)t + \theta_n]}_{\text{upper modulation lines}} + \underbrace{\frac{A_0'a_n}{2} \operatorname{Cos}[(2\pi f_0 - \rho_n)t + \theta_n]}_{\text{lower modulation lines}}. \end{aligned} \tag{12}$$

It can be seen that each modulating frequency $\rho_n/2\pi$ will produce a pair of modulation lines separated from the f_0 carrier by frequencies $\pm\rho_n/2\pi$, respectively. It will be possible to see these lines on the coherent spectrum analyzer.

B. Angle Modulation

In the process of amplification in the transmitter, the time function (3) is delayed by some time, D. If this time delay D is itself a function of time, an angle modulation of $f(t)$ will occur.

$$f(t + D(t)) = A_0' \operatorname{Cos}[2\pi f_0(t + D(t))]. \tag{13}$$

$D(t)$ may be divided into D_0, the fixed delay, and $d(t)$, the delay variation.

$$f(t + D(t)) = A_0' \operatorname{Cos}[2\pi f_0(t + D_0 + d(t))] \tag{14}$$

absorbing D_0 into t, $t' = t + D_0$

$$f(t' + d(t)) = A_0' \operatorname{Cos} [2\pi f_0(t' + d(t)]. \quad (15)$$

For a time-delay variation $d(t)$ represented by a sum of sinusoidal components

$$d(t) = \sum_{n=1}^{n=M} a_n \operatorname{Cos} (\rho_n t + \theta_n) \quad (16)$$

where $\rho_n/2\pi$ is the frequency of the nth component, and θ_n is the constant part of its phase,

$$f(t' + d(t)) = A_0' \operatorname{Cos} \left[2\pi f_0 t' + \sum_{n=1}^{n=M} 2\pi f_0 a_n \operatorname{Cos} (\rho_n t + \theta_n) \right]. \quad (17)$$

$2\pi f_0 a_n$ represents the maximum instantaneous phase shift for any modulating frequency $\rho_n/2\pi$. For modulation components which are well below the carrier, $2\pi f_0 a_n$ is small. For $(2\pi f_0 a_n) < 0.2$

$$\begin{aligned} f(t' + d(t)) &\cong A_0' \{ \operatorname{Cos} (2\pi f_0 t) \\ &- \pi f_0 a_1 \operatorname{Sin} [(2\pi f_0 + \rho_1)t + \theta_1] - \pi f_0 a_1 \operatorname{Sin} [(2\pi f_0 - \rho_1)t - \theta_1] \cdots \\ &- \underbrace{\pi f_0 a_n \operatorname{Sin} [(2\pi f_0 + \rho_n)t + \theta_n]}_{\text{upper modulation lines}} - \underbrace{\pi f_0 a_n \operatorname{Sin} [(2\pi f_0 - \rho_n)t - \theta_n]}_{\text{lower modulation lines}} \}. \end{aligned} \quad (18)$$

It can be seen that in this case also, each modulating frequency $(\rho_n/2\pi)$ will produce a pair of modulation lines separated from the f_0 carrier by $\pm(\rho_n/2\pi)$, respectively. It will be possible also to see these lines on the coherent spectrum analyzer.

An interesting case occurs when both amplitude and angle modulation are present in about equal amounts and are derived from the same modulating frequency. The amplitude and angle modulation components will add vectorally. The amplitude modulation components possess even phase symmetry about the f_0 line while the angle modulation components possess odd-phase symmetry about f_0 line. For certain values of phasing between the amplitude and angle modulation, modulation components on one side of the f_0 line will cancel while modulation components on the opposite side will reinforce. This will produce a nonsymmetric modulation line distribution about the f_0 line.

C. *Pulse-Repetition Rate Modulation*

The foregoing analysis has dealt with the effects of gain and time-delay variation as a function of time of an amplifier on a microwave pulse train. These modulation mechanisms operate on all lines in the pulse spectrum, and hence inspection of the region about the f_0 spectral line is sufficient to reveal all modulation lines in the spectrum.

For amplifiers which are also used to gate the pulse out of the carrier, another modulation mechanism occurs. It was assumed in the previous analysis that the pulse-repetition rate (F) was stable, or at least the instability was not introduced by the amplifier under test. Where the input to the amplifier is simply f_0 and the amplifier performs the gating function to produce the spectrum as given in (1), the pulse-repetition rate (F) can introduce interline modulation if it is not stable. For an unstable PRF

$$F(t) = F_0 + F'(t); \quad (19)$$

$$H(f) = AF(t)t_0 \left[\sum_{n=-\infty}^{n=\infty} \delta[(f - f_0) - nF(t) \right] \cdot \frac{\operatorname{Sin} \pi t_0(f - f_0)}{\pi t_0(f - f_0)}. \quad (20)$$

The amplitude variation represented by $AF(t)t_0$ is small for values of $F'(t)$ small with respect to F_0. The frequency of the f_0 line of the spectrum corresponding to $n = 0$ is unaffected by PRF instability, but the frequency of succeeding PRF lines is modulated by the nth multiple of $F'(t)$. To preserve spectral line purity for any appreciable number of PRF lines, $F'(t)$ must be very small. This requires a high-stability PRF source. Modulation occurring due to PRF instability can be observed on the coherent analyzer.

III. Methods of Spectrum Analysis

A. *The Noncoherent Panoramic Analyzer*

The usual panoramic spectrum analyzer is a narrowband receiver tunable over a wide frequency range with provisions for frequency sweeping portions of the tuning range. The analyzer CRT display is calibrated vertically in amplitude and horizontally in frequency.

In analyzing a microwave pulse spectrum the analyzer first converts the microwave signal to a fixed IF frequency by heterodyning with an internal tunable transfer oscillator. Depending on the final filter bandwidth the analyzer may contain several more down-frequency converters. One of these conversion oscillators will be swept in frequency in order to move the pulse spectrum across the final filter in the analyzer.

The final filter tuning stability is limited by the stability of the internal transfer oscillators. A secondary limitation is also imposed by the filter time constant in relation to the total frequency swept, and the sweep time. The sweep must be slow enough to remain on a spectral line for at least one filter time constant to charge the filter. Where the total frequency range to be swept is wide, and the filter is narrow, long sweep times are incurred. A more fundamental limitation on final filter bandwidth is transfer oscillator instability. To produce a good stable IF signal for filter charging, the combined instabilities in the transfer oscillators should not exceed a peak frequency deviation of about 10 per cent of the filter bandwidth. For most microwave spectrum analyzers, transfer oscillator instability limits the filter bandwidth to about 5 kc. Many transmitter systems operate with a PRF rate of less than 2 kc. This means that spectral lines will be separated by less than 2 kc. The 5-kc resolution of the commercial microwave spectrum analyzer cannot resolve this line structure. The pattern displayed on this type of analyzer shows the envelope of spectral lines. A pseudo-line structure is sometimes observed in this envelope display. These lines are not the spectral lines of the $H(f)$ pulse-frequency spectrum but are lines generated by the interaction of the signal PRF and the analyzer sweep rate. They will be stationary in the pattern when the analyzer sweep is synchronized to the signal PRF. An example of such a display is shown in Fig. 2. These pictures were taken on a video analyzer after coherent translation of the microwave signal to 11 Mc. At this frequency the transfer oscillators in the video spectrum analyzer had enough stability to allow a filter width of about 100 cps. Effects of the transfer oscillator instability are apparent in the third and fourth photographs (Fig. 2) of the series showing the spectrum line structure. The last two pictures in the series were taken on the coherent analyzer and show the line resolution possible when an all-coherent chain is used.

B. Coherent Conversion

Where microwave amplification devices are being tested, as opposed to microwave signal source testing, it is not important to know the stability of the signal source driving the amplifier except as it is affected by transmission through the amplifier. It is possible, by use of a low-frequency stable oscillator and an up-conversion process, to produce a microwave signal whose stability is a function of a set of conversion oscillators. This microwave signal may be used to drive the amplifier under test. The microwave output of the amplifier is reconverted to the stalo-oscillator frequency using the same conversion oscillators as were used for the up conversion. This coherent conversion technique separates the microwave drive-signal instability from the modulation and instability introduced by the amplifier under test. Fig. 3 shows a typical coherent converter. A stable low-frequency f_s is converted to a microwave frequency f_0 in three up conversions:

$$f_0 = f_s + f_1 + f_2 + f_3. \tag{21}$$

f_0 is gated to form a pulse spectrum $H(f)$. It will suffice to trace only a single frequency component, in this case f_0, through the amplifier and down-conversion process to demonstrate the instability canceling of the coherent converter. Where Δf is the sum of modulation products and instabilities introduced by the amplifier under test, the amplifier output f_M is

$$f_M = f_0 + \Delta f = [f_s + f_1 + f_2 + f_3 + \Delta f]. \tag{22}$$

f_M is reconverted to a base-frequency f_s in the down converter.

$$f_M - (f_1 + f_2 + f_3) = f_s + \Delta f. \tag{23}$$

Thus the pulse spectrum $H(f)$ has been converted to a low-frequency base f_s, but the modulation Δf on each spectral line has been retained. From this base frequency further noncoherent conversion and filtering will allow use of a very narrow frequency analyzer filter. The last two pictures on Fig. 2 show spectral lines viewed with such a filter.

C. Filters and Frequency Transfer

The narrow bandwidth filter, approximately 2 cps in width, used as the final analyzer filter usually has a center frequency in the order of 10 kc to 100 kc. For narrower bandwidth filters this center frequency becomes lower. The microwave signal to be inspected must be translated to this frequency and swept across the filter. The energy in a microwave signal spectrum is distributed over a frequency range of several megacycles. In order to prevent folding of this spectrum about zero frequency as the spectrum center frequency is translated to a lower base frequency, filters must be incorporated before each conversion to limit the bandwidth to less than twice the new base frequency. At the lower base frequencies crystal filters are used. Fig. 4 shows a set of photographs taken at sampling points in the down-converter chain. They demonstrate time-delay and band-pass filtering characteristics. Fig. 5 shows a block diagram of a low-frequency, noncoherent converter designed to translate an 80-kc bandwidth signal spectrum on a 1.5-Mc base frequency to a 4-kc bandwidth signal on a 2.5-kc base frequency. At this point a conventional audio analyzer provides the final filter, display and sweeping circuits. A stepped crystal transfer oscillator allows positioning of any portion of the 80-kc signal bandwidth in the 4-kc crystal-filter bandwidth. This feature makes possible inspection of any portion of the 80-kc signal bandwidth. Transfer oscillators are crystal controlled to provide the necessary stability as required by the final analyzer filter.

D. The Coherent Analyzer

The coherent analyzer constructed (see Fig. 6) had a −3-db filter bandwidth of less than 2 cps with filter skirts 30-cps wide at the −50-db points. The usable dynamic range of the analyzer was 50 db. The analyzer was able to inspect a frequency range ±2 kc about the f_0 carrier frequency. The analyzer was intended as a tool for checking UHF and L-band radar transmitters. It supplied coherent pulsed signal at IF to the transmitter exciter. The exciter converted this pulsed IF signal to UHF or L-band frequency by heterodyning it with a high-stability local oscillator. The coherent analyzer sampled this UHF or L-band signal at points along the transmitter chain. These sampled signals were reconverted to IF in a crystal mixer using a sample of the exciter stalo as the conversion oscillator. The test signal was coherently converted to a 1.5 Mc center frequency

Sweep rate synchronized to PRF.

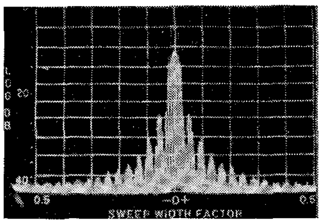

Sweep rate not synchronized to PRF.

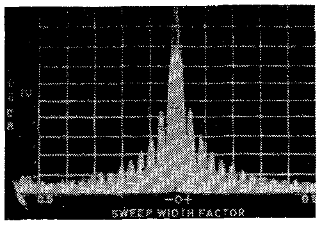

Sweep width factor = 50 kc/cm.
Display scale: log.

Sweep rate synchronized to PRF.
False line structure
Due to sweep PRF interaction.

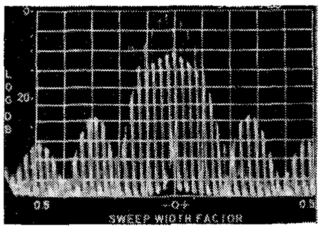

Sweep rate not synchronized to PRF.

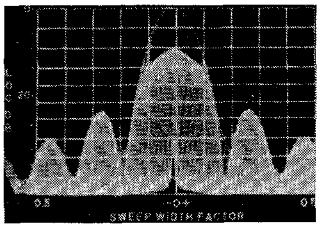

Sweep width factor = 10 kc/cm.
Display Scale: Log.

Series shows development of discrete line structure in spectrum display.

Sweep width factor; 10 kc/cm.
Display: log.
Analyzer adjusted for fine resolution.

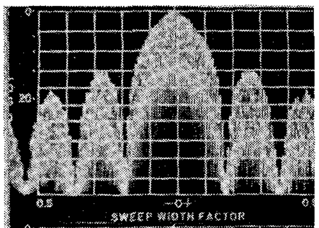

Sweep width factor: 1 kc/cm.
Analyzer showing center lobe.

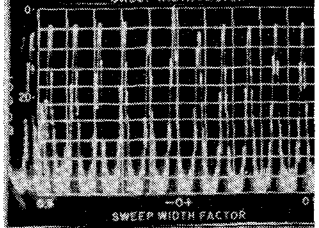

Sweep width factor: 200 cps/cm.
Analyzer showing f_0 and $f_0 \pm 1$-kc lines.

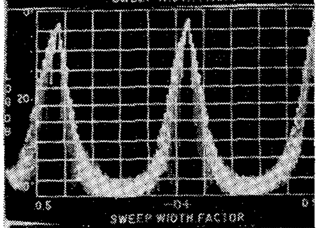

Sweep width factor: 100 cps/cm.
Analyzer showing f_0 line.
Frequency instability due to analyzer noncoherent operation.

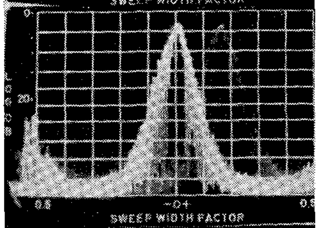

Coherent analyzer display.
Sweep width factor: 20 cps/cm.
Analyzer showing f_0 line.

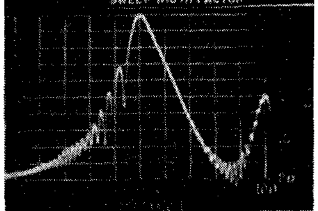

Coherent Analyzer Display
Sweep width factor: 2 cps/cm.
Analyzer showing f_0 line.

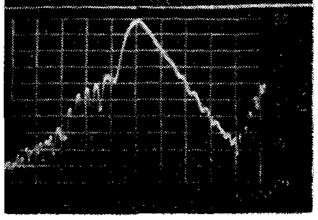

Fig. 2—Spectrum display of 40 μsec, 1-kc PRF pulse train.

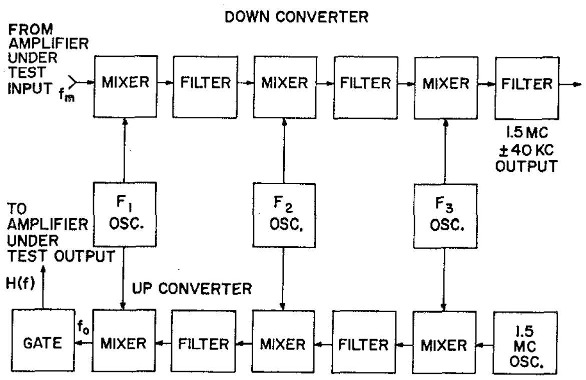

Fig. 3—Coherent frequency converter block diagram.

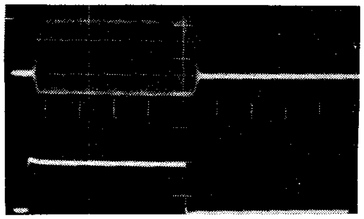

Top: 11 Mc sample (partial detection due to scope).
Bottom: 60 Mc detected pulse.
Vertical: 0.05 v/cm.
Horizontal: 10 μsec/cm.

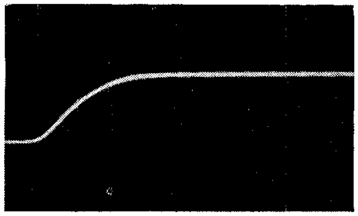

Rise time: 60 Mc detected pulse.
Vertical: 0.05 v/cm.
Horizontal: 0.1 μsec/cm.

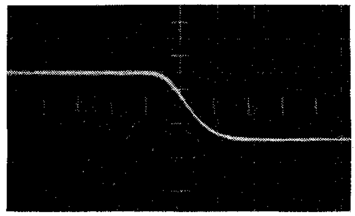

Fall time: 60 Mc detected pulse.
Vertical: 0.05 v/cm.
Horizontal: 0.1 μsec/cm.

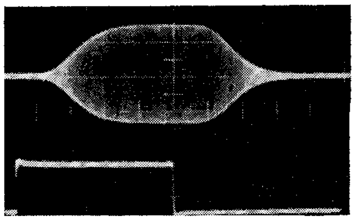

Top: 1.5 Mc sample.
Bottom: 60 Mc detected envelope.
Vertical top: 0.2 v/cm.
Vertical bottom: 0.05 v/cm.
Horizontal: 10 μsec/cm.

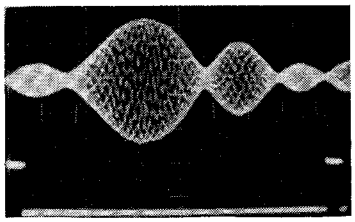

Top: 3 kc sample.
Bottom: 60 Mc detected envelope.
Vertical top: 2 v/cm.
Vertical bottom: 0.05 v/cm.
Horizontal: 100 μsec/cm.

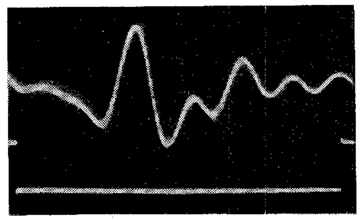

PRF synced to RF to show wave form structure.

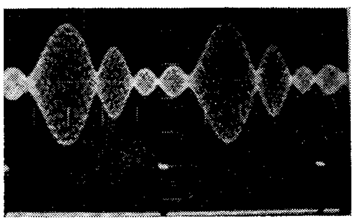

Top: 3 kc sample.
Bottom: 60 Mc detected envelope.
Vertical top: 2 v/cm.
Vertical bottom: 0.05 v/cm.
Horizontal: 200 μsec/cm.

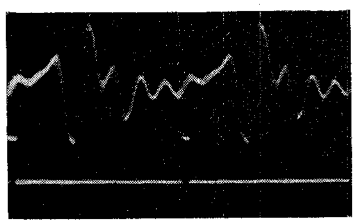

Fig. 4—RF and detected waveforms showing progress of pulse through down-frequency converter of coherent spectrum analyzer.

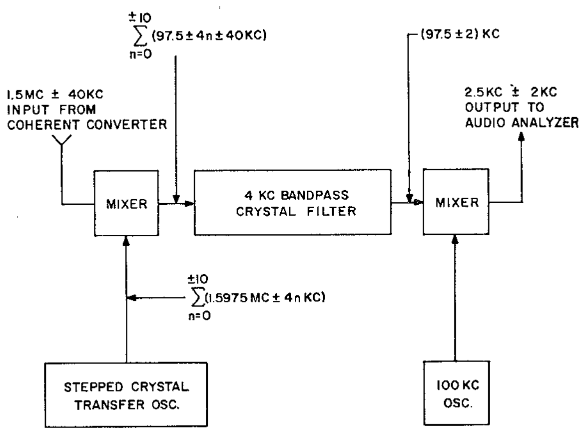

Fig. 5—Noncoherent-frequency converter block diagram.

and from there was noncoherently converted to a 2.5-kc center frequency. In the down-conversion process the signal was filtered to a bandwidth of 4 kc. The 4-kc wide signal centered at 2.5 kc was displayed on an audio spectrum analyzer. The analyzer was modified to drive a chart recorder for permanent record readout. The recorder readout was used for most of the transmitter testing. As was mentioned before the sweep speed is limited by the analyzer resolution. In order to charge a filter having a 2-cps bandwidth, a sweep rate less than 0.5 sec per 1 cps is required. A little over half an hour is required to sweep the full 4 kc at this sweep rate. For this operation the recorder is most useful. Once the general modulation content of the 4-kc region has been determined, the analyzer sweep can be narrowed to

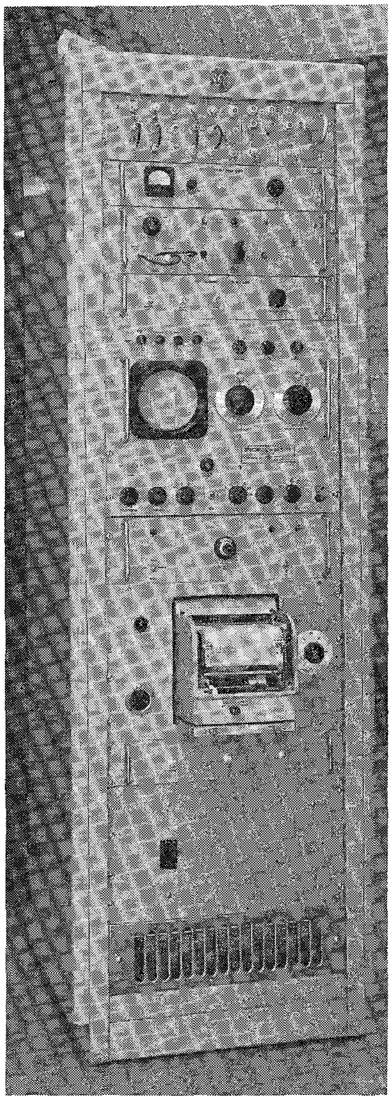

Fig. 6—Spectrum analyzer cabinet.

display interesting portions of the 4-kc region in a shorter time period. Results of tests conducted to date have shown that the regions ± 150 cps about the f_0 and PRF spectral lines contain the greatest amount of modulation and noise. The interline areas outside of these regions have largely been found free of noise and modulation products.

IV. Modulating Mechanisms in Microwave Amplifiers

As was noted previously, all modulation in microwave amplifiers arises from either gain or time-delay variation of the amplifier. This produces modulation lines about each spectral line of the pulse spectrum. In the special case where the amplifier is also used as the pulse gate or where amplifier video drive is pulsed and does not bracket the RF pulse, modulation and jitter of the PRF lines is possible when the gating action is unstable.

Each of the three generally used microwave amplifiers, the klystron, the TWT and the conventional gridded tube, has some special modulation problems. Some modulation problems are shared by all three. Power supply ripple and mechanical vibration account for most of the modulation lines found in the fine grain spectrum of an amplified pulse. Modulation product frequencies for systems operating from a 60-cps supply line are 60 cps for ac heater and half-wave rectifier systems. 120-cps ripple occurs in full-wave rectifier systems, while 360-cps and 720-cps ripple frequencies occur in high-power three-phase power supplies. These ripple frequencies either amplitude or angle modulate the pulse spectrum. The type of modulation depends on the modulation mechanism in effect. Mechanical vibrations may also be based on power line frequencies where they arise from rotating or vibrating ac machinery such as transformers and blowers. In other cases mechanical vibration is excited by air or water coolant flow.

A. Traveling-Wave Amplifiers

The traveling-wave amplifier depends on the interaction of an electron beam and a slow-wave structure to produce amplification. This interaction occurs over several wavelengths thereby making the tube electrically long. As such it is quite sensitive to time-delay, or phase, modulation. Power supply ripple on electrodes affecting the electron beam velocity or shape will modulate the beam which will in turn phase modulate the amplified signal. Focus-coil power-supply ripple and filament electric and magnetic fields may also modulate the beam. Mechanical vibration of the tube may change the electrode spacings and the helix-beam position. The time delay of a TWT is more sensitive to these disturbances than is the gain. Hence, most of the modulation components added to a signal by a traveling-wave amplifier will be phase modulation.

B. Klystron Amplifiers

Klystrons are similar to traveling-wave amplifiers in their modulation sensitivities. The electron beam in the klystron is sensitive to collector and modulating anode ripple voltages and to focusing field modulation caused by ripple current in the focus coils. Under certain conditions, filament excitation may also cause beam modulation. In high-power klystrons which require considerable coolant flow, mechanical vibrations in the cavities caused by coolant flow will introduce phase modulation into the signal spectrum. Ion oscillation may also introduce modulation lines into the spectrum.

C. Triodes, Tetrodes, and Other Gridded Tubes

Various gridded tubes are used in the lower microwave frequency regions. These tubes operate with external tuned elements. Modulation mechanisms in these tubes are quite different from those of klystrons and traveling-wave amplifiers. The tube electrical path length is short compared to a TWT or klystron, thereby reducing the possibility of phase modulation. Tube gain, however, is dependent on the dc operating point. AC ripple on plate, screen and bias supplies will vary the gain, and hence, will amplitude modulate the signal. In high-power tubes where filaments, rather than heater-cathodes are used, dc filament excitation must be used to minimize amplitude modulation. The external cavities on these tubes are also a source of both phase and amplitude modulation. When a tuning element vibrates, the signal transmitted through the cavity will be phase modulated. If the cavity is tuned to the exact center frequency of the microwave signal, little amplitude modulation will occur as a result of element vibration. If, however, the cavity is tuned slightly off the signal frequency, vibration of tuning elements will cause the signal to traverse the steep slope of the bandpass curve. This will produce a considerable amount of amplitude modulation.

Most of these modulation mechanisms have been observed in fine grain spectrum measurements made on several transmitter systems using TWT's, klystrons and gridded tubes. Some examples of measurements made are presented in the next section.

V. Examples of Microwave Spectrum Measurements

The results of three spectrum tests are presented to demonstrate the modulation mechanisms previously discussed.

A. Modulation Due to Cavity Vibration

A three-stage UHF exciter consisting of a mixer and two-tetrode cavity amplifiers was found to have an excessive amount of 60-cps and 56-cps modulation in the output signal spectrum. It was possible to minimize the modulation by careful tuning of the cavities. Fig. 7 shows a series of spectrum runs taken about the f_0 spectral line after the modulation was minimized by tuning. The 56- and 60-cps modulation levels were not repeatable between runs. Cross modulation between the 56- and 60-cps modulation lines was suspected. The spectrum about the upper PRF line was inspected. The PRF line itself was jittery due to the relatively unstable PRF source used for testing, but the 56- and 60-cps modulation lines were still present. (See Fig. 8.) A sample of the signal taken from the output of the mixer before the RF amplifiers was analyzed (Fig. 8, Chart 3). No 56- or 60-cps modulation lines were found. This isolated the modulation to the RF amplifiers. The air blowers contributed to the 56-cps modulation. To check on the cross modulation between the 56-cps and the 60-cps lines, the analyzer was manually set on the 60-cps line, and the chart recorder was allowed to run. The amplitude of the 60-cps line varied with time at a 4-cps rate. The air blower was shut off, and the 60-cps line amplitude variation stopped. (See Fig. 9.) The analyzer was reset to the 56-cps modulation line. It also showed the cross-modulation effect with the 60-cps line. When the blower was turned off the 56-cps line disappeared. Investigation of the RF amplifier cavities showed that a tuning plate was free to vibrate. Transformer lamination vibration and vibration caused by air blower imbalance (56 cps due to induction motor slip) excited vibration in the tuning plate. Balancing of the air blower, tightening of the transformer laminations and damping the tuning plate eliminated the 56- and 60-cps modulation lines in the exciter output (Fig. 9, Chart 3).

B. Modulation in an L-Band Transmitter

An L-band transmitter system using a tetrode-cavity exciter, a traveling-wave amplifier driver and a klystron-amplifier output was tested using the coherent spectrum analyzer. Low ripple power supplies were used throughout the transmitter. Some ac filaments were used. After transmitter debugging final spectrum runs were made on the f_0 line and the first upper PRF line of the spectrum. (See Figs. 10 and 11.) The transmitter output spectrum contained no modulation lines above -50 db, except at 60 cps. At 60 cps the exciter introduced modulation lines; the TWT driver and klystron amplifier added to these lines bringing the final modulation level in the transmitter to -45 db. The modulation was not symmetric about the f_0 or PRF lines. Hence it was determined that the modulation consisted of both amplitude and phase modulation in about equal amounts and phased to produce partial cancellation of the energy in one sideband. During testing the transmitter was operated on a local trigger source of relatively low stability. The jitter on the PRF line (Fig. 11) reflects this instability.

C. PRF Instability

To demonstrate the effects of PRF instability on the spectral line structure, the coherent analyzer was connected in a closed loop at a frequency of 60 Mc. In closed loop the pulsed output of the up-frequency converter is fed to the input of the down-frequency converter. The pulse gate was triggered by a Hewlett-Packard Model 212-A pulse generator. Fig. 12 shows the spectral line structure of the f_0 line and the upper two PRF lines. For this test the PRF used was 1 kc. The HP-212-A pulse generator introduced an appreciable amount of frequency jitter to the line structure. After these spectrum runs were made a General Radio NO-1100A Frequency Standard with an output at 1 kc was used to lock the PRF of the HP-212-A pulse generator. The spectral line series as shown in Fig. 12 was rerun with the locked PRF. Fig. 13 shows these results. The results demonstrate the necessity of providing a stable PRF for systems in which fine grain spectral purity is a requirement.

VI. Conclusion

This paper has described the design and operation of a fine line spectrum analyzer capable of inspecting the interline regions of a pulsed microwave frequency spectrum. The coherent conversion technique used, while not new in itself, is new to the field of microwave spectrum analysis. The analyzer which was constructed was used primarily for high-power radar system testing. The analyzer and the principles it embodies should be equally useful in developing any microwave amplifier device or system where energy in the fine grain microwave spectrum must be measured and controlled.

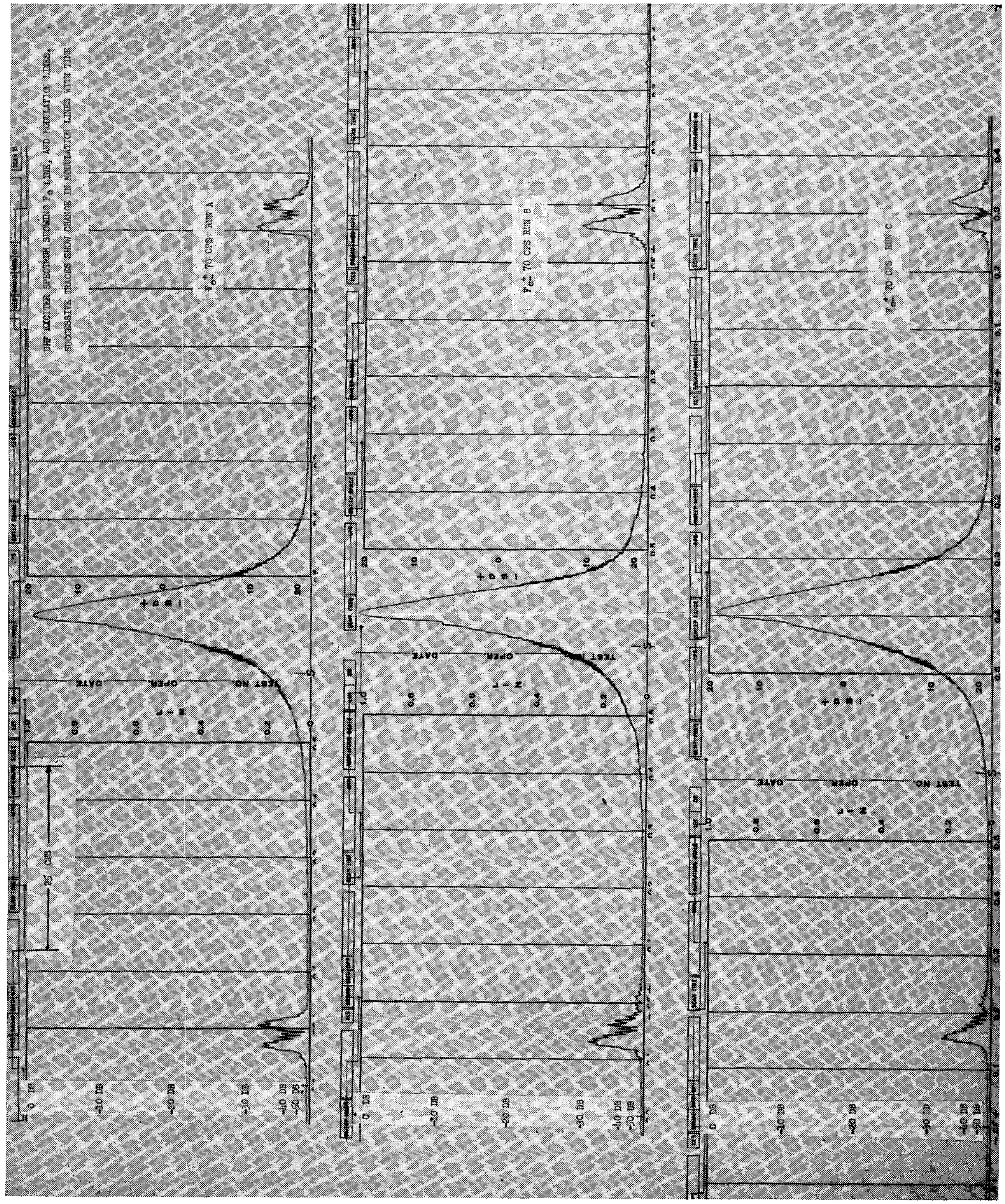

Fig. 7.

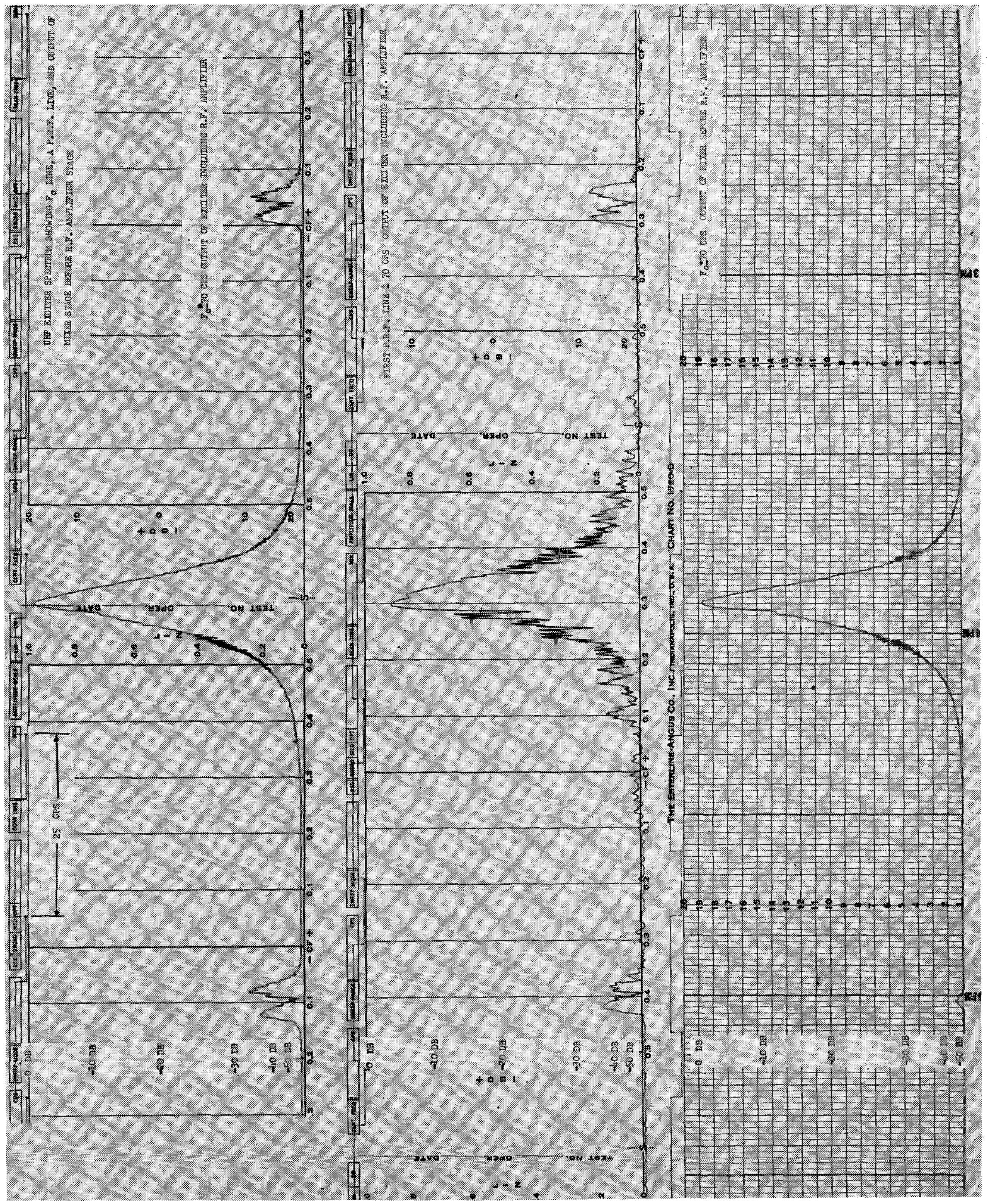
UHF EXCITER SPECTRUM SHOWING F0 LINE, A P.R.F. LINE, AND OUTPUT OF MIXER STAGE BEFORE R.F. AMPLIFIER STAGE
25 CPS
FIRST P.R.F. LINE ± 70 CPS OUTPUT OF EXCITER INCLUDING R.F. AMPLIFIER
0 DB
-10 DB
-20 DB
-30 DB
-40 DB
-50 DB

Fig. 8.

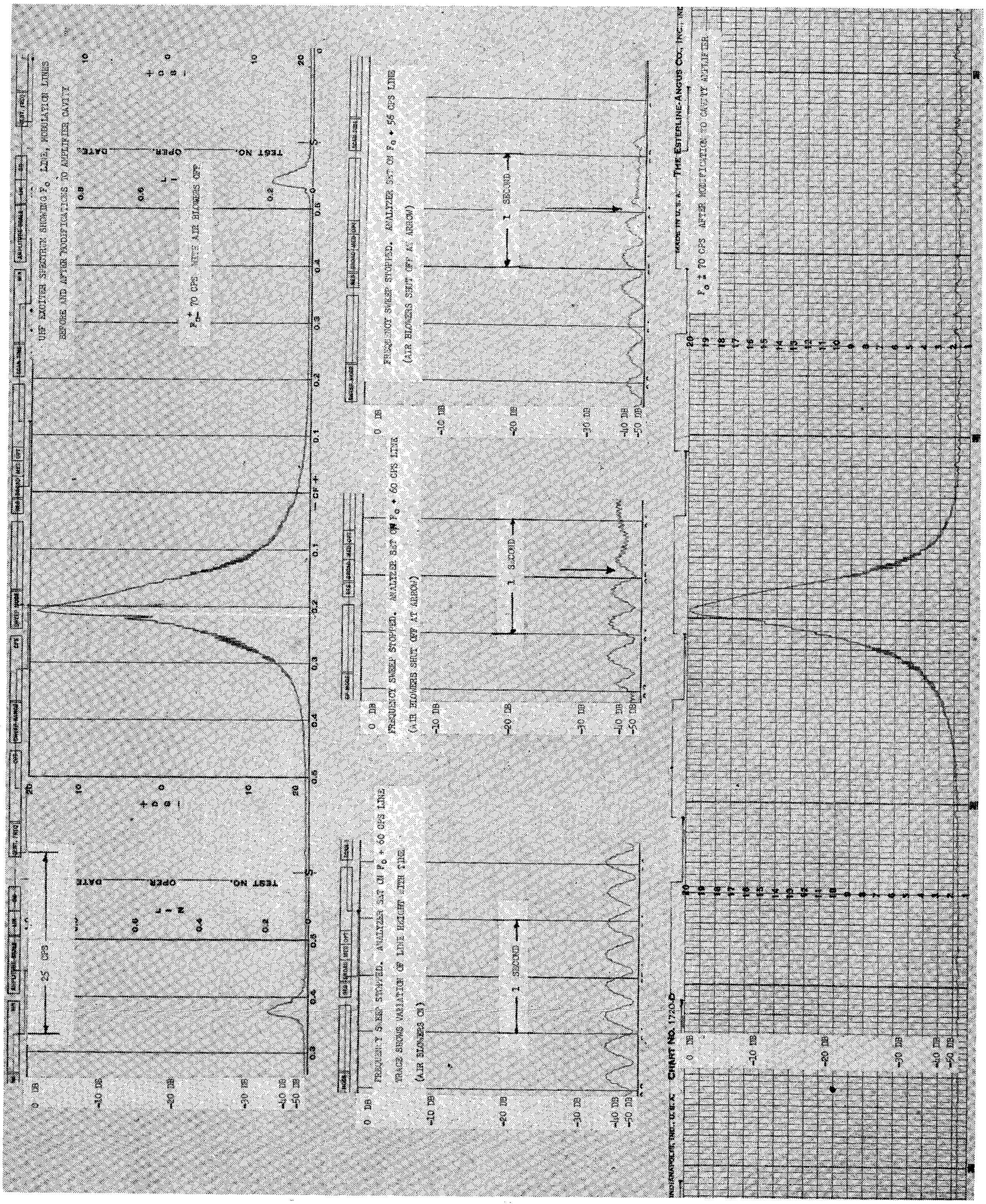

Fig. 9.

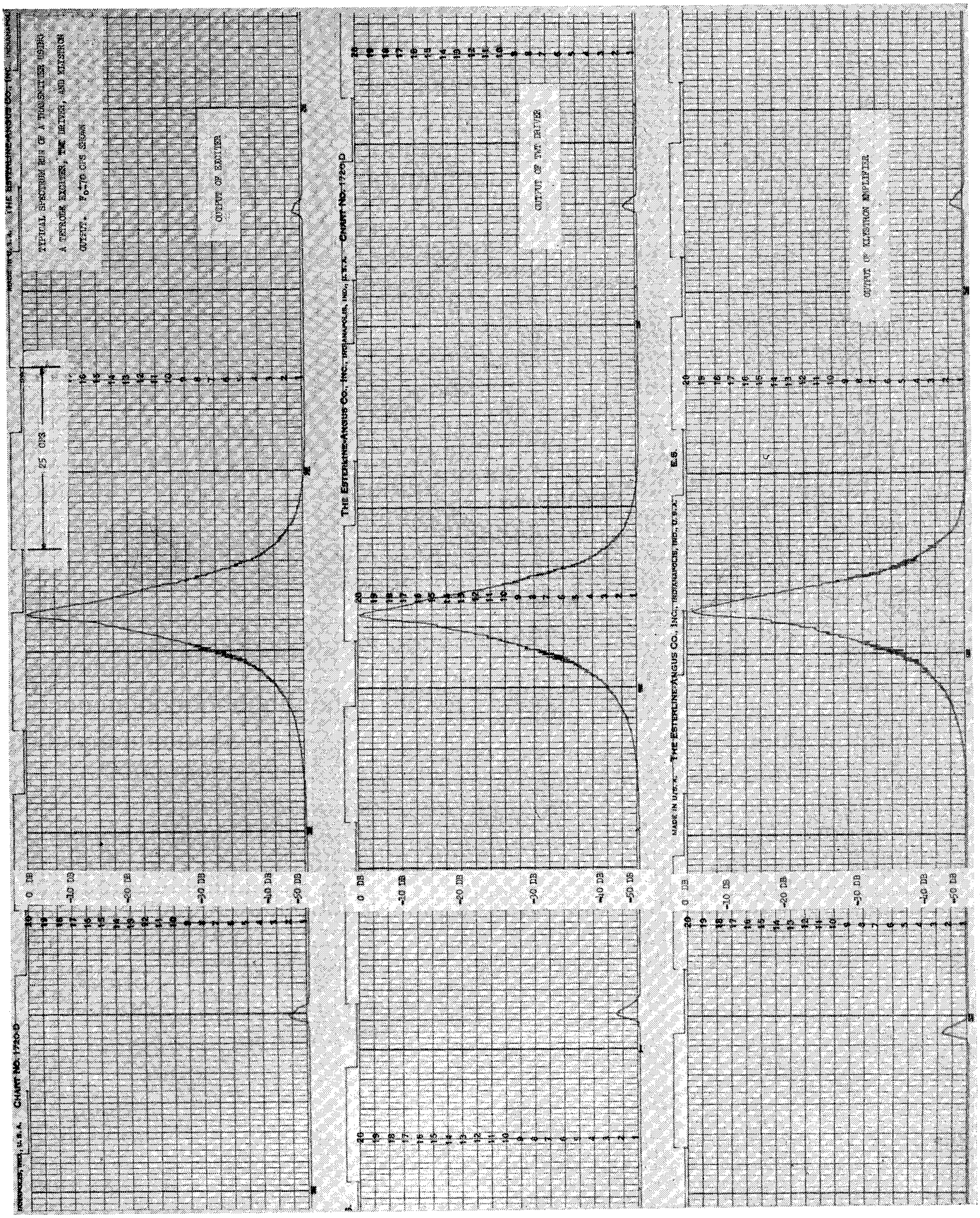

TYPICAL SPECTRUM RUN OF A TRANSMITTER USING A TETRODE EXCITER, TWT DRIVER, AND KLYSTRON OUTPUT.
OUTPUT OF EXCITER
25 CPS
OUTPUT OF TWT DRIVER
OUTPUT OF KLYSTRON AMPLIFIER
0 DB
-10 DB
-20 DB
-30 DB
-40 DB
-50 DB

Fig. 10.

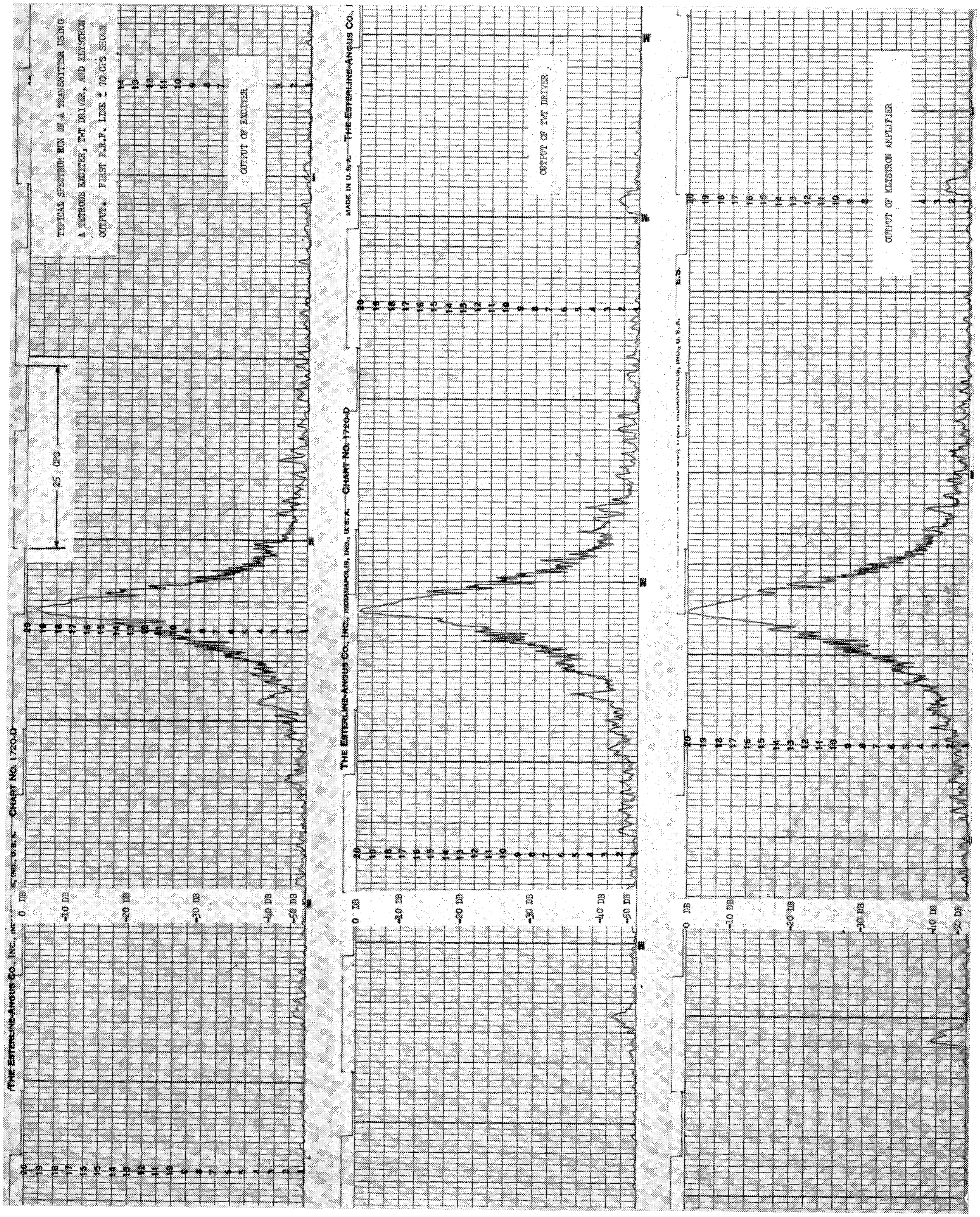
TYPICAL SPECTRUM RUN OF A TRANSMITTER USING
A TETRODE EXCITER, TWT DRIVER, AND KLYSTRON
OUTPUT OF EXCITER
OUTPUT OF TWT DRIVER
OUTPUT OF KLYSTRON AMPLIFIER
25 CPS
0 DB
-10 DB
-20 DB
-30 DB
-40 DB
-50 DB
THE ESTERLINE-ANGUS CO., INC.
CHART NO. 1720-D

Fig. 11.

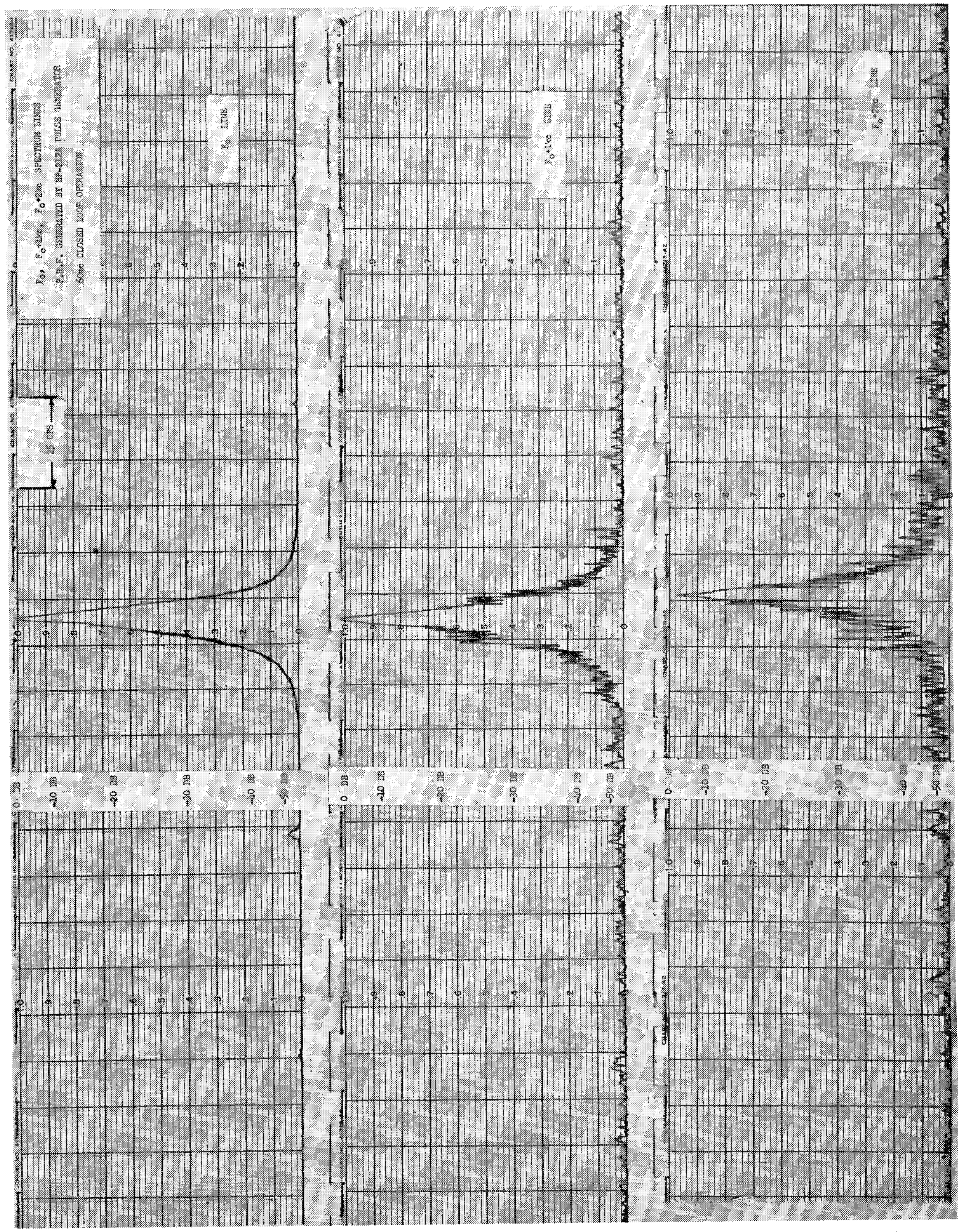
F0, F0+1kc, F0+2kc SPECTRUM LINES
P.R.F. GENERATED BY HP-212A PULSE GENERATOR
60mc CLOSED LOOP OPERATION
25 CPS
F0 LINE
F0+1kc LINE
F0+2kc LINE

Fig. 12.

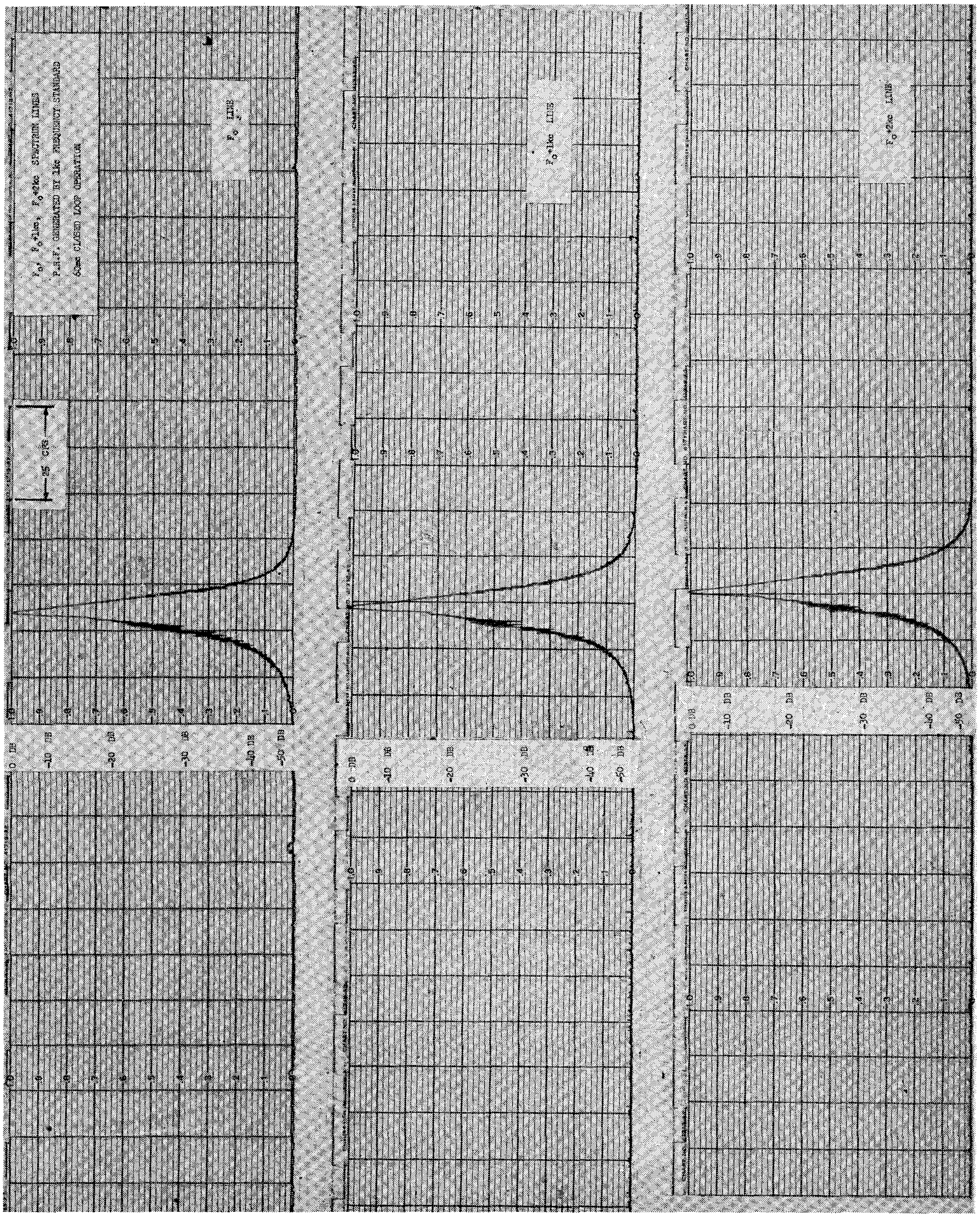

Fig. 13.